M a t h e m a t i c a
B a l k a n i c a

New Series Vol. 20, 2006, Fasc. 1

Case Studies in Solving the PDF for Particular Fluid Dynamics Problems

Zoran Markov [1] *and Predrag Popovski* [2]

Presented at Conference on "PDE Methods in Appl. Math. and Image Proc."

The solution of the fluid flow field requires solving the conservation equations for mass and momentum. For flows involving heat transfer or compressibility, an additional equation for energy conservation needs to be solved. The objective of this article is to demonstrate the accuracy of the numerical (CFD) analysis in prediction of the fluid flow cases and turbomachinery performances. A comparison with the experimental data is made, which will later be used as a powerful tool in the design process.

AMS Subj. Classification: 30C45

Key Words: Univalent, starlike, strongly starlike of

1. Introduction

The difficulties in solving the PDF equations in fluid dynamics have proved in the past as one of the factors for the slower development of numerical approach in the design of hydraulic turbomachinery. Lately, because of the extremely fast computers and their affordability, this approach is getting more applicable than ever, which was not the case until recently. Of course, we still need the reliability of the numerical solutions to replace the physical model testing, which is significantly more expensive and time demanding. The benefit of the results and data acquired using CFD methods, enable more efficient development of hydraulic machinery, which is reflected on the power generation, as well on the environmental impact.

2. Numerical Modeling and Governing Equations

The prediction of the flow field in fluid dynamics requires solving the conservation equations for mass and momentum. For flows involving heat transfer

or compressibility, an additional equation for energy conservation is solved. Additional transport equations are also solved when the flow is turbulent. The conservation equations for laminar flow (in a non-accelerating reference frame) are presented. The equation for conservation of mass, or continuity equation, can be written as follows:

$$\frac{\partial \rho}{\partial t} + \frac{\partial (\rho u_i)}{\partial x_i} = S_m$$

This equation is the general form of the mass conservation equation and is valid for incompressible as well as compressible flows. The source S_m is the mass added to the continuous phase from the dispersed second phase (e.g., due to vaporization of liquid droplets) and any user-defined sources.

Conservation of momentum in the i-th direction in a internal (non-accelerating) reference frame is described in [1]:

$$\frac{\partial (\rho u_i)}{\partial t} + \frac{\partial (\rho u_i u_j)}{\partial x_j} = -\frac{\partial p}{\partial x_i} + \frac{\partial (\tau_{ij})}{\partial x_j} + \rho g_i + F_i$$

Equations for conservation of mass, momentum, energy, and species and other scalar equations sometimes have to be solved in time-dependent form. Activating time dependence is sometimes useful when attempting to solve steady-state problems, which tend toward instability (e.g., natural convection problems in which the Rayleigh number is close to the transition region). It is possible in many cases to reach a steady-state solution by integrating the time-dependent equations.

Time-dependent equations must be discretized in both space and time. The spatial discretization for the time-dependent equations is identical to the steady-state case. Temporal discretization involves the integration of every term in the differential equations over a time step Δt.

The integration of the transient terms is straightforward, as shown below. A generic expression for the time evolution of a variable ϕ is given by $\frac{\partial \phi}{\partial t} = F(\phi)$, where the function F incorporates any spatial discretization. If the time derivative is discretized using backward differences, the first-order accurate temporal discretization is given by

$$\frac{\phi^{n+1} - \phi^n}{\Delta t} = F(\phi)$$

and the second-order discretization is given by

$$\frac{3\phi^{n+1} - 4\phi^n + \phi^{n-1}}{2\Delta t} = F(\phi)$$

where ϕ - a scalar quantity; $n+1$ - value at the next time level $t+\Delta t$; n - value at the current time level t; $n-1$ - value at the previous time level $t-\Delta t$.

Once the time derivative has been discretized, a choice remains for evaluating $F(\phi)$: in particular, which time level values of ϕ should be used in evaluating F?

One method is to evaluate $F(\phi)$ at the future time level. This is referred to as "implicit" integration since ϕ^{n+1} in a given cell is related to ϕ^{n+1} in neighboring cells through $F(\phi^{n+1})$:

$$\phi^{n+1} = \phi^n + \Delta t F(\phi^{n+1})$$

The advantage of the fully implicit scheme is that it is unconditionally stable with respect to time step size. A second method is available when the coupled explicit solver is used. This method evaluates $F(\phi)$ at the current time level and is referred to as "explicit" integration since ϕ^{n+1} can be expressed explicitly in terms of the existing solution values, ϕ^n :

$$\phi^{n+1} = \phi^n + \Delta t F(\phi^n)$$

Here, the time step Δt is restricted to the stability limit of the underlying solver (i.e., a time step corresponding to a Courant number of approximately equal to 1). In order to be time-accurate, all cells in the domain must use the same time step. For stability, this time step must be the minimum of all the local time steps in the domain. The use of explicit time stepping is fairly restrictive. It is used primarily to capture the transient behavior of moving waves, such as shocks, because it is more accurate and less expensive than the implicit time stepping methods in such cases [4].

The conventional techniques described earlier both implicit and explicit, use artificial viscosity terms, which must be specifically chosen and tuned for a particular problem. If strong shocks are present, employment of large numerical dissipation may obscure the real physics. One of the efforts to overcome this problem is the development of upwind schemes [9]. This has been applied to both implicit [10] and explicit [11] techniques. Upwind schemes are attractive because they provide a rational mathematical framework for adding dissipation to a scheme. The may be more robust than schemes with artificial viscosity. The do not usually have operator prescribed constants. Most of the techniques described earlier use conservative central difference schemes to capture shocks, requiring arbitrary smoothing parameters (artificial dissipation) to stabilize the calculation. The upwind difference schemes are used to capture strong shocks without requiring arbitrary parameters, which may alter the physics of the prob-

lem. The flux evaluation is numerically more intensive in upwind schemes; the scheme is more complicated to code and requires more computational time.

3. Turbulence Modeling

In general, the flow in turbomachinery passages is turbulent and needs to be modeled as such, therefore the turbulence models are an important component of any CFD code.

Turbulent flows are characterized by fluctuating velocity fields. These fluctuations mix transported quantities such as momentum, energy, and species concentration, and cause the transported quantities to fluctuate as well. Since these fluctuations can be of small scale and high frequency, they are too computationally expensive to simulate directly in practical engineering calculations. Instead, the instantaneous (exact) governing equations can be time-averaged, ensemble-averaged, or otherwise manipulated to remove the small scales, resulting in a modified set of equations that are computationally less expensive to solve. However, the modified equations contain additional unknown variables, and turbulence models are needed to determine these variables in terms of known quantities.

Standard CFD codes usually provide the following choices of turbulence models:

- Spalart-Allmaras model
- Standard $k - \epsilon$ model
- Renormalization-group (RNG) $k - \epsilon$ model
- Realizable $k - \epsilon$ model
- Reynolds stress model (RSM)
- Large eddy simulation (LES) model.

It is a fact that no single turbulence model is universally accepted as being superior for all classes of problems. The choice of turbulence model will depend on considerations such as the physics encompassed in the flow, the established practice for a specific class of problems, the level of accuracy required, the available computational resources, and the amount of time available for the simulation. To make the most appropriate modeling for your application, you need to understand the capabilities and limitations of the various options.

4. Comparison of the Numerical Results and Experimental Data

In this paper, several case studies for incompressible fluid, as well as two and three-dimensional models of simple and more complex geometry are presented.

4.1. Hydrodynamic and cavitation performances of modified NACA hydrofoil

The flow is calculated for several different angles of the modified NACA 4418 hydrofoil and in different flow regimes. However, two main regimes have been calculated using numerical solution of the governing PDE for the flow field (TASCflow code [5]), one where the cavitation does not occur, and one where it does and it must be taken into account. Cavitation is a process of evaporation of the water at low pressure values. For the purpose of determining the flow parameters around a single hydrofoil, including cavitation process, a cavitation tunnel has been used. The tunnel used in the experimental work is located at the research laboratory at the Turboinstitut-Ljubljana [6].

The results that have been obtained indicate that, although other models have some advantages concerning stagnation point paramters etc, the best turbulence model for this case is the $k-\epsilon$ standard (or default) model. The following analysis and calculations are performed using this turbulence model [2].

Comparison of the results for lift and drag coefficients is shown in the following table

	Experiment		TASCflow $k-\epsilon$	
Non-cavitation regime, α^0	lift	drag	lift	drag
0	0.44	0.020	0.45867	0.01586
4	0.80	0.035	0.91070	0.02166
8	1.22	0.046	1.31382	0.03020
12	1.50	0.070	1.58110	0.06448
16	1.65	0.140	1.79700	0.09264
Cavitation regime, α^0				
0	0.44	0.020	0.45867	0.01586
4	0.80	0.035	0.83314	0.02166
8	1.20	0.080	1.26425	0.06763
12	1.36	0.200	1.34534	0.12174
16	1.36	0.320	1.37307	0.19990

The cavitation occurance has also been analysed for several angles of

attack. The length of the cavitation cloud taken as a non dimensional value over the cord length (Xc) is taken as a comparison factor for this analysis. The graphical presentation of the TASCflow results and photos from the experiment, as well as corresponding values of Xc for $\alpha = 8^0$ are presented in the following Figure 1.

Figure 1. Cavitation photo and TASCflow presentation of cavitation at $\alpha = 8^0$

The next table shows the comparison of the results for cavitation cloud length.

α^0	Experiment	TASCflow
8	0.33	0.29
12	0.60	0.71
16	0.64	0.60

Simulation of unsteady flow using FLUENT CFD [4] code shown in the following figure 2 presents the cavitation inception and development at angle of attack of 12^0 at time step of 0.4 ms; 1.0 ms; 24.2ms; and 74.2 ms.

Several conclusions can be drawn from this case:

- Results for cavitation tunnel of a hydrofoil profile showed some differences for the hydrodynamic parameters, when different turbulence closure models where used, although these differences (in the worst case) didn't exceed 5 percent for the value of the lift coeffcient
- The same model showed pretty good compatibility for the prediction of the pressure distribution (pressure coeffcient) around the blade for several angles of attack (different positions of the equipment)
- Lift and drag coefficients for several angles of attack were calculated, and the greater angles of attack again showed some differences corresponding with the experimental results, which is crucial in the design process of the system

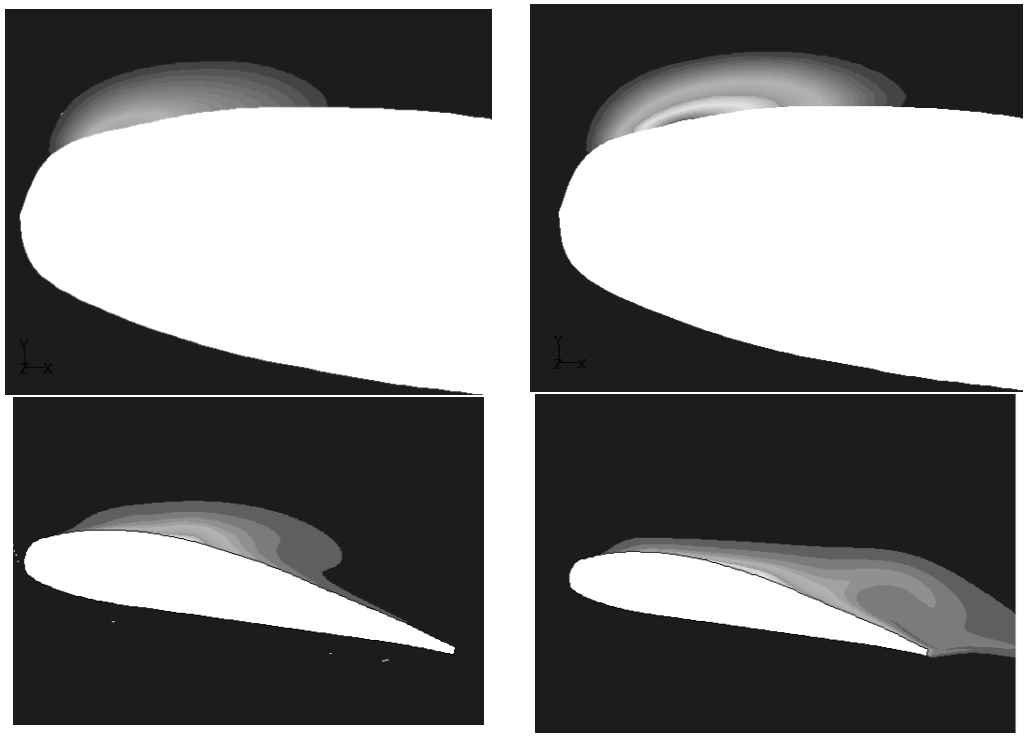

Figure 2. Cavitation inception and development at angle of attack of 12^0 at time step of 0.4 ms; 1.0 ms; 24.2ms; and 74.2 ms.

- Cavitation was modelled using the models currently available in TASCflow (CEV) and in FLUENT (Cavitation) and they showed some good predictions for the length of the cavitation cloud, which can cause severe damage to the parts of the turbomachinery

4.2. Cavitation performances of pump-turbine

The calculated flow area of the pump-turbine was meshed by means of volume element method. The next figure 3 shows the complete flow area for the calculated pump turbine. The meshing of the flow field is also presented in this figure. The number of calculating elements that are used by the TascFlow code reaches over one million. The optimal number of these elements is hard to be set having in mind the time needed for the calculation as well as the accuracy that is required.

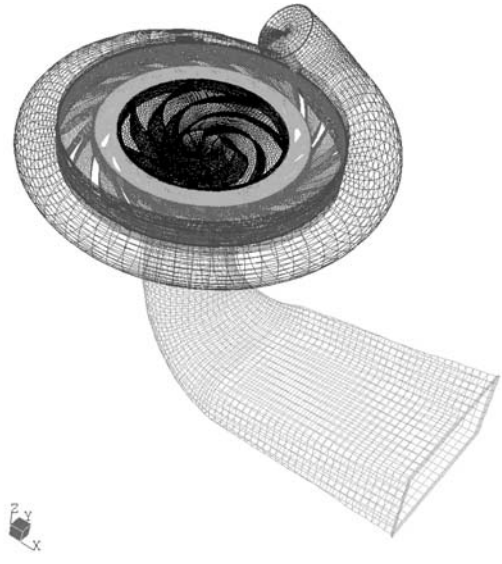

Figure 3. The complete flow area for the pump-turbine

Specific parameter for the calculation is the definition of the boundary condition for the rotor. In this case a boundary condition Frozen rotor was used. In both methods, numerical and experimental, cavitation was calculated using overall cavitation coefficient of the machine σ [8]. The results of the calculation are presented by efficiency drop and visualization of vapor inception at inlet edges of the impeller vanes. Figure 4 presents two calculated points at different inlet pressure values. The figure on the left shows optimal pump mode without cavitation. The other figure presents increase of the vapor phase at impeller blades.

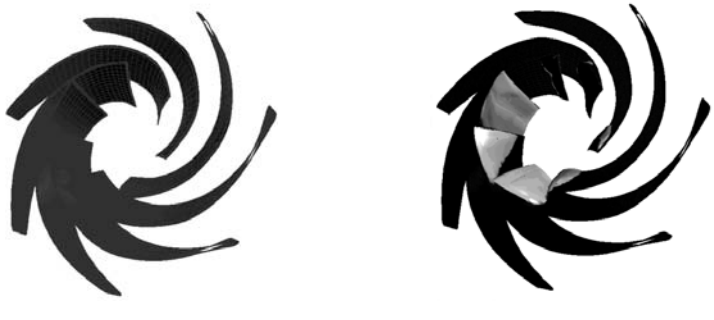

Figure 4. Optimal pump mode without cavitation (on the left) and increase of the vapor phase at impeller blades at off-design point (on the right)

In the next figure 5, the comparison of the calculated and experimental efficiency drop due to the cavitation is presented.

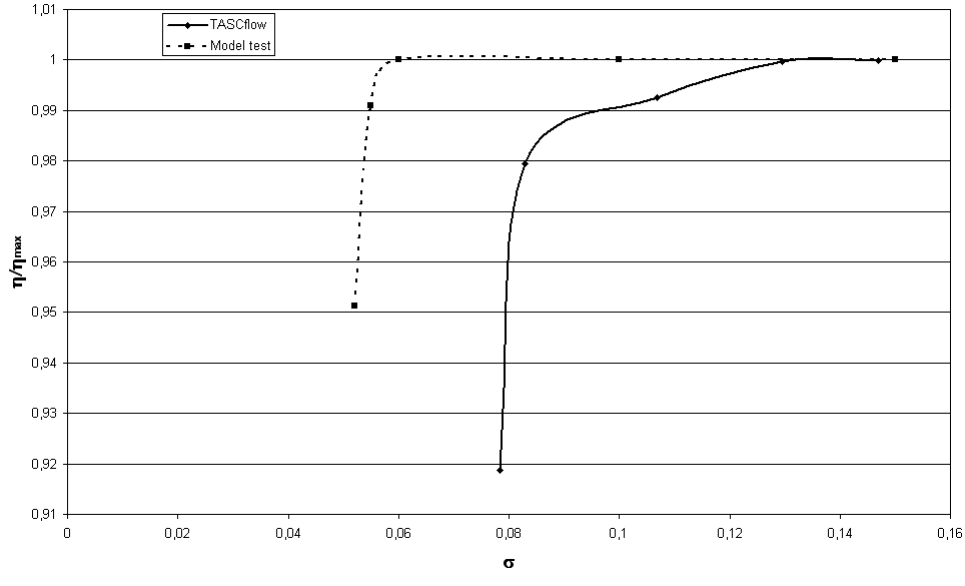

Figure 5. Comparison of the calculated and experimental efficiency drop due to the cavitation

The $x-$axis in this figure represents the cavitation coefficient $\sigma = (p_{st} - p_v)/(\rho v^2/2)$ and the $y-$axis represents the relative decrease in the efficiency of the pump-turbine.

This example coincides with the current trend of application of the CFD methods as a faster and less expensive way of development in hydraulic machinery. The results are promising, but a lot of experiments are still necessary for the completion of the validation process.

The influence of the cavitation on the total efficiency is calculated for the pump mode. Using these results, conclusions regarding the exploitation and design processes can be achieved.

Relatively significant discrepancy between the CFD code results and the experiment shows that further investigation is needed to achieve higher accuracy of the numerical prediction. The numerical model predicts the occurrence of cavitation somewhat earlier than the actual physical model on the test rig. Several factors could lead to this result, but the most important ones, certainly include the description of the physical model (not just as simple two-phase flow), geometry definition may still need some improvement because of the small areas where the cavitation occurs, as well as the effects of the secondary flow.

References

[1] Batchelor, G.K., *An Introduction to Fluid Dynamics*, Cambridge Univ. Press, Cambridge, England, 1967

[2] Launder B.E. and Spalding D.B., *Lectures in Mathematical Models of Turbulence*, Academic Press, London, England, 1972.

[3] Wilcox D.C., *Turbulence Modeling for CFD.* DCW Industries, Inc., La Canada, California, 1993.

[4] *FLUENT 5 Guide*, Fluent Inc, 1998.

[5] *AEA, Advanced Scientific Computing*, CFX-TASCflow, ver. 2.10 - Primer, Waterloo, Canada, 2000.

[6] Vujanic V., Raziskava toka okoli lopate namescene v kavitacijskem tunelu, Magisterij, Univerza v Ljubljani, Fakulteta za strojnistvo, Ljubljana, 1992.

[7] Markov Z. et al., CFD modeling and simulation of cavitation in water conduits,In: *IFAC Automatic Systems for Building the Infrastructure in Developing Countries Proceedings*, Istanbul, Republic of Turkey,77-82, 2003.

[8] Popovski P. et al., Numerical three-dimensional turbulent flow analysis through a pump-turbine draft tube in the turbine mode,In: *Proceedings of the International Conference Hydro 2003*, Cavtat, Croatia, Vo. I, 333-340, 2003.

[9] Osher S. and Solomon F., Upwind schemes for hyperbolic systems of conservation laws, *Math. Comput.*, **38**, 1982, 239.

[10] Rai M. M. and Chakravathy S. R., An implicit form for the Osher upwind scheme, *AIAA J.*, **24**, 1986, No. 5, p.735.

[11] Chakravathy S. R. and Osher S., Numerical experiments with the Osher upwind scheme, *AIAA J.*, **21**, 1983, No. 9, p.1241.

Department of Hydraulic Engineering and Automation
Faculty of Mechanical Engineering
Karpos II b.b., 1000 Skopje
R. Macedonia
[1] *E-mail: mzoran@mf.ukim.edu.mk*
[2] *E-mail: predrag@mf.ukim.edu.mk*

Received 31.01.2005